APPLYING THE PRESSURE DERIVATIVE METHOD TO IDENTIFY GEOTHERMAL WELL RESPONSES

Katie McLean[1]* and Sadiq J. Zarrouk[1]

[1]Department of Engineering Science, University of Auckland, New Zealand

*pmcl037@aucklanduni.ac.nz

Keywords: *Pressure transient analysis, well testing, pressure derivative, SAPHIR™, downflow, geothermal wells.*

ABSTRACT

The pressure derivative method is one of the most significant developments in the history of pressure transient analysis (PTA). PTA results that would otherwise be difficult to interpret can have a clear and characteristic pressure derivative. The application of this technique in groundwater, coalbed methane, mineral exploration and oil and gas wells has been widespread. However their application in the well test analysis of geothermal wells is still very limited.

The usefulness of the pressure derivative technique is demonstrated in this study. Despite the challenges of geothermal wells it remains a key diagnostic tool to determine the processes taking place during the test and hence the models which might be applicable.

Two common issues with applying PTA to geothermal wells are 1) downflows and 2) non-zero flow early in the pressure falloff (PFO) test. Downflows of fluid from a higher permeable zone to a deeper one of lower pressure can occur during the test. Non-zero flow can occur due to the delay inevitable when manually closing a master valve.

For each issue of downflow and early non-zero flow some real examples are given. The characteristic anomalies these effects produce in a derivative plot are presented along with a discussion of the extent to which these issues affect the results obtained by treating these as standard analyses.

1. INTRODUCTION

The cornerstone of the pressure derivative method is the derivative plot, a specialized graph which allows a reservoir engineer to "diagnose" the test. There are many different analytical models which are relevant in early, intermediate and late-time. In combination these models can in theory reproduce the entire shape of the field data. The "diagnosis" of a test is the selection of models that are chosen. This is done based on the characteristic shape(s) of the field data displayed in a derivative plot. The derivative plot is therefore the starting point of the analysis. Then the variables relevant to the chosen model(s) can be manipulated in an attempt to match the model results to the field data – an inverse modelling process.

The derivative plot has been applied widely in the oil and gas industry, where PTA is often successful in obtaining a good match with field data. In geothermal wells there are many significant differences to oil and gas testing (detailed in Section 2.2). These challenges have limited the application of the derivative plot and PTA in the geothermal industry where results from PTA are considered with justified skepticism. In the majority of cases PTA produces results which are inconsistent and do not fit the field data well.

There are many geothermal effects the render the application of PTA difficult if not impossible. In this study we look at two very common issues present in geothermal well tests: 1) downflows and 2) non-zero flow early in a PFO test. The characteristic appearance of these in a derivative plot is presented both as real field data and models using the SAPHIR™ commercial well test analysis software. The impact of these effects on the results of analysis is investigated.

2. BACKGROUND

2.1 Pressure derivative method

The pressure derivative method is also called the Bourdet derivative and was introduced in 1983 around the time of the advent of computers (Bourdet et al., 1983; Bourdet et al., 1989; Bourdet, 2002). The method is a significant advance that has greatly enhanced modern PTA (Horne, 1995; Houzé et al., 2012)

The cornerstone of the method is the derivative plot which is the slope (derivative) of the semi-log plot (Figure 1a) represented on the log-log plot (Figure 1b).

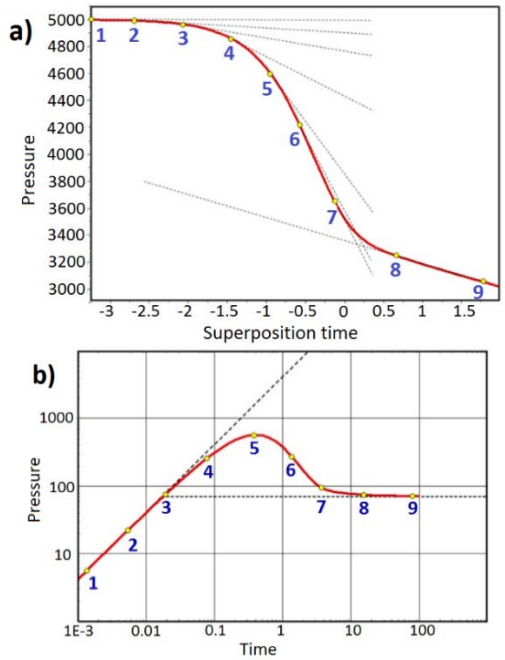

Figure 1: Derivative plot example: a) points of various slopes on the semilog plot and b) those same points represented in a log-log plot (reproduced with kind permission of KAPPA Engineering)

Figure 1 shows the simple example of a well with storage and skin which starts in the storage flow regime with a unit slope (Figure 1b: between points 1-3) before transitioning

to a period of infinite-acting radial flow (IARF) with a slope of zero (Figure 1b: between points 8-9).

The derivative method was originally developed in order to better identify the IARF flow period which has a characteristic flat derivative (Figure 1b; Figure 2). The method turned out to be useful far beyond this original scope. Many different flow regimes and well, reservoir and boundary behaviours have a characteristic shape on the derivative plot (Figure 2) (Houzé et al., 2012).

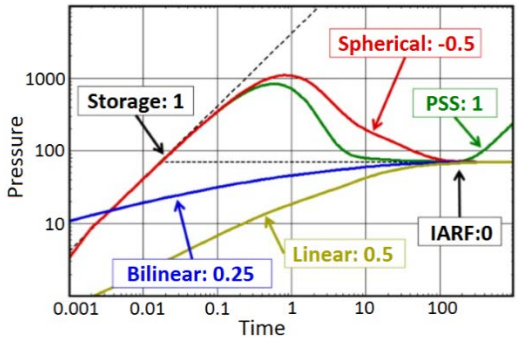

Figure 2: Characteristic shapes of various flow regimes on a derivative plot and their associated characteristic slopes (reproduced with kind permission of KAPPA Engineering)

2.2 Limitations of PTA in geothermal fields

The diffusivity equation is the source of all analytical models. Each analytical model is a solution to the diffusivity equation given here in radial coordinates (Earlougher, 1977; Horne, 1995):

$$\frac{\partial^2 p}{\partial r^2} + \frac{1}{r}\frac{\partial p}{\partial r} = \frac{\emptyset \mu c_t}{k}\frac{\partial p}{\partial t} \qquad (1)$$

The assumptions made in the derivation of this linear equation as stated by Earlougher (1977) are:

1. Horizontal flow
2. Negligible gravity effects
3. Homogeneous and isotropic porous medium
4. Single fluid with small/constant compressibility
5. Darcy's Law applies
6. Fluid and reservoir properties (μ, c_t, k, ∅) are independent of pressure.

Geothermal reservoirs are not isothermal and so fluid properties are not uniform throughout the reservoir (O'Sullivan et al., 2005). Those fluid properties depend non-linearly on thermodynamic conditions (pressure, temperature, saturation, composition). They are particularly variable when boiling and condensation are occurring. Therefore assumptions 4 and 6 in the above list do not apply to geothermal wells/reservoirs.

Grant and Bixley (2011) highlight the point that geothermal reservoirs are usually in volcanic rock where permeability is controlled by faults/fractures in a three dimensional network that is connected to the wellbore only at limited points. Therefore assumptions 1 and 3 also do not apply as flow will be in any direction through the network not just the horizontal direction and the system is anything but homogenous.

Technically the linear diffusivity equation (1) must therefore be replaced with a non-linear form which requires numerical models to solve (Earlougher, 1977; O'Sullivan et al. 2005).

The assertion is made by Grant and Bixley (2011) that despite the invalidity of the assumptions of the diffusivity equation, the application of PTA theory derived from this equation to geothermal wells is often successful in practice. Regardless of the true frequency of successful geothermal PTA analyses it is clear that the application of PTA theory to geothermal wells must be done with extreme caution. This is with a clear understanding of the manner in which the assumptions are breached, with an intent to compensate for the deviation if possible.

3. RESULTS AND DISCUSSION

The software SAPHIR™ is used to present the pressure vs time data from various well tests. A variety of analytical models are available to fit the field data. SAPHIR™ automatically generates a history plot, semi-log plot and derivative plot.

3.1 ISSUE 1: DOWNFLOWS

3.1.1 WK44/0 Background

This shallow monitoring well is in the western borefield of Wairakei geothermal field in New Zealand. Despite being a "groundwater" well it reaches temperatures of 110°C and has more than one permeable zone. WK44/0 is 44m deep, cased to 6m and with an average groundwater level of around 18m. Every year students of the University of Auckland Geothermal postgraduate certificate program perform an injection/pressure- fall-off (PFO) test. Every year the PFO begins normally and then exhibits a kink in the data approximately 30 minutes into the test at which time the rate of pressure decline appears to slow down (Figure 3).

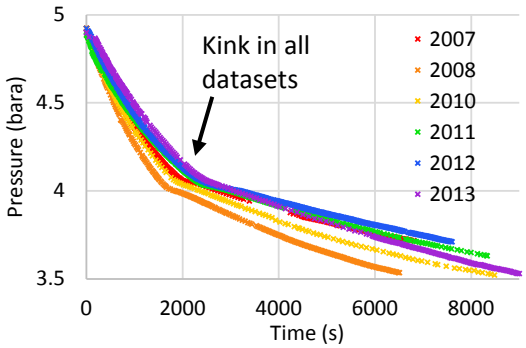

Figure 3: Pressure vs time for some PFO tests on WK44/0 for 2007-2013.

3.1.2 WK44/0 derivative plot

The derivative plot for the 2010 dataset is typical of all years and shows a small dip in the derivative (Figure 4). No models exist which will model a dip such as this. For example a model fit for radial flow in a homogeneous infinite acting reservoir cuts through the dip.

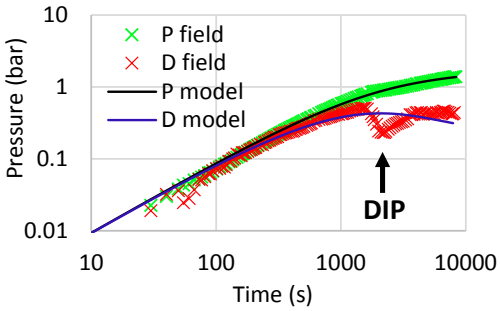

Figure 4: Derivative plot of WK44/0 PFO in 2010. Pressure data is green, pressure derivative is red and the thin lines overlying these are the SAPHIR™ model fit (Model 1 of Table 1).

This characteristic derivative shape in Figure 4 at first glance resembles the dip of a dual-porosity response. However the dip of a dual-porosity response is much broader (Horne, 1995). This WK44/0 response has the width of approximately 0.5 log cycles. In general features less than 0.5 log cycles would be considered to be spurious (Horne, 1995), however that conclusion is not possible here as the same response is observed over many tests.

3.1.3 Scenario 1: Fracture closing

It is necessary to think beyond standard analytical models. One hypothesis is that this response represents a change in permeability during the test - a fracture which was stimulated during injection and then closed again as pressure dropped below fracture pressure during the PFO. This hypothesis would account for the "slowing down" of the pressure decline after the kink. However this is not consistent with what is known about the injection history. The injection is set up in the afternoon and the amount of water accepted by the well decreases overnight by around 50% and the well is always overflowing the next day. If the well is stimulated by injection and fractures are opening then the amount of water accepted should be more and not less as injection proceeds.

3.1.4 Scenario 2: Secondary shallow permeable zone

Another hypothesis is that there is a shallow permeable zone in this well which is usually dry and above the local water table. During injection this zone becomes saturated after which it accepts less water. During the PFO as the water level in the well drops below this zone, it begins to flow back into the well. This would add to the water column and give the appearance that the water level was going down more slowly (Figure 5).

The kink appears around 30 minutes into the tests, when the water level is around 9m below casing head flange (CHF). The casing in this well is 6m from CHF leaving 3m in which to find this permeable zone. Evidence of this zone is seen in temperature profiles during early injection (Figure 6). During injection temperature increases more rapidly with depth over permeable zones as cold injected water exits the wellbore. The data in Figure 6 does indicate a very minor permeable zone around 9-12m in addition to the major permeable zone from 18-37m.

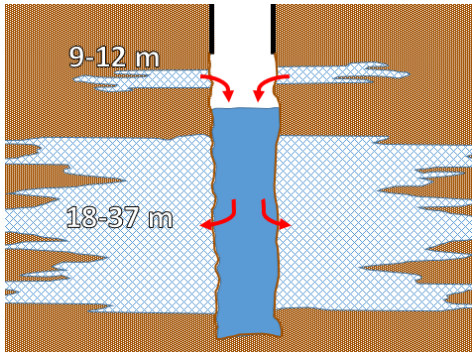

Figure 5: Schematic in well during PFO for Scenario 2: Secondary shallow permeable zone.

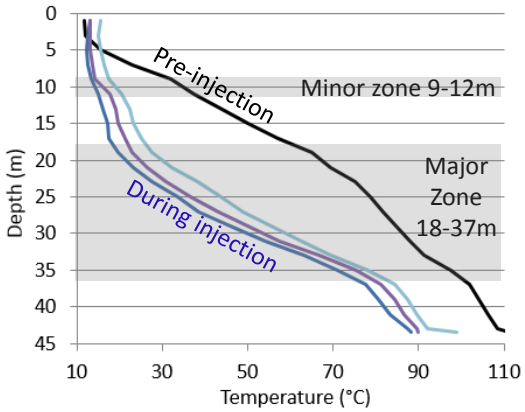

Figure 6: Temperature profiles for WK44/0 both prior to and during injection in 2011.

3.1.5 Non-standard SAPHIR™ analysis

To match a model to the data it is not valid to include data from after the kink as it is affected by the downflow. Including this data will give a very poor model match which does not reproduce the kink (Figure 4, Table 1: Model 1). Altering regression points to ignore the affected data is not enough as they still affect the match through the time history (Figure 7, Table 1: Model 2). The affected data must be deleted (Table 1: Model 3) however as so few data points remain the model is poorly constrained. The model can be constrained using the infinite-acting reservoir pressure (Pi) which is known from the groundwater level prior to the test (Figure 8, Table 1: Model 4). A summary of the various models is given in Table 1 and Figure 9.

Table 1: SAPHIR™ model parameters summary

	Model 1	Model 2	Model 3	Model 4
	All data included	Regression points altered	Data deleted	Model 3 with Pi imposed
k (mD)	1.42	1.05	5.69	2.26
kh (mD.m)	55.4	41	222	88.3
s	-3.26	-3.32	6.68	-0.812
Pi (bara)	2.97	2.34	3.34	3.01
C (m^3/bar)	0.0518	0.0597	0.0648	0.0623

*All models are for a homogenous infinite acting reservoir

The parameters which define each model (Table 1) are:

- k – reservoir permeability (units: mD)
- kh – reservoir permeability-thickness product (units: mD.m))
- s – skin factor (dimensionless)
- Pi – infinite acting pressure (units: bara)
- C – wellbore storage coefficient (units: m^3//bar)

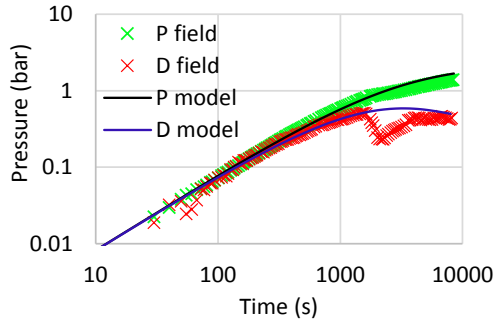

Figure 7: Derivative plot of Model 2 (Table 1). Match improved by deleting regression points.

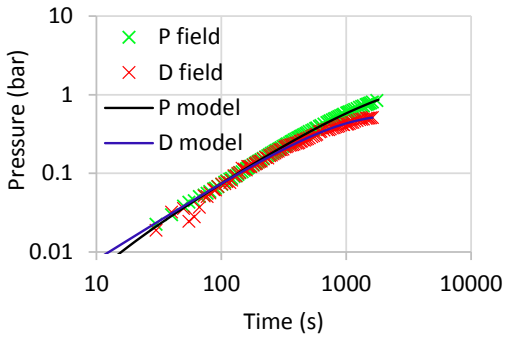

Figure 8: Derivative plot of Model 4 (Table 1) - looks identical to Model 3. Match improved by deleting data points and model constrained with Pi.

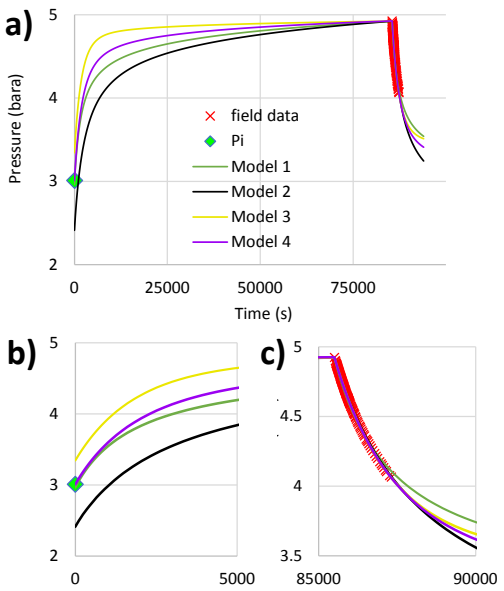

Figure 9: a) History plot of Models 1-4 (from Table 1) with close-ups of b) early injection and c) PFO.

With an acceptable model obtained, the downflow can be modelled by the following method:

- Alter the rate history to add a period of injection flow starting at the time of the kink.
- Regenerate the simulation while retaining the existing model parameters and then export the time history.
- Repeat these steps for a range of injection flows.
- Graph results for all injection flows together (Figure 10)

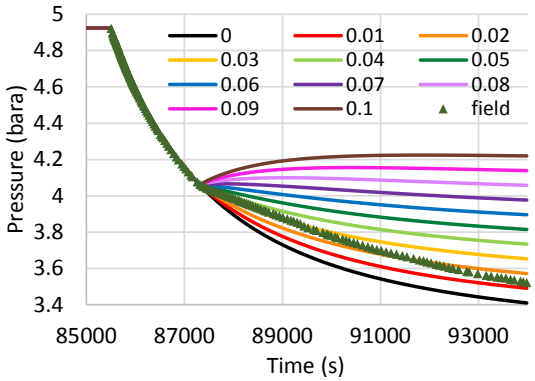

Figure 10: History plot of downflow modelling: no downflow (black), increasing magnitude downflows 0.01-0.1 m^3/h (rainbow colours), compared to field data (green points).

The time histories of Figure 10 indicate that a scenario consistent with the field data would be a downflow of around 0.04m^3/h starting at the time of the kink and reducing to nearly 0.01 m^3/h over the rest of the PFO interval. This range 0.04-0.01 m^3/h (0.01-0.003 L/s) is a very small flow and quite plausible.

3.1.6 Multilayered well response discussion

The example of WK44/0 represents an important example of what a geothermal multi-layered well response can look like. This is new PTA territory as in oil and gas wells it is uncommon to be testing multiple layers. Oil and gas reservoirs are typically stratigraphic and more importantly the wells are only perforated at one permeable zone (or if at multiple zones, these zones are tested separately using packers). Geothermal reservoirs are significantly different as they are often not stratified and everything below the casing shoe is 'perforated' liner. This entire open-hole section of a geothermal well is being tested at once and this is often >1000m and with multiple feed zones.

The scenario of multiple permeable layers connected to the wellbore and also to each other in an oil and gas reservoir is called 'crossflow' (Horne, 1995). The pressure transient response in such cases frequently looks like a normal single-layer response, or sometimes a dual-porosity response if there is a big difference in thickness or skin between the layers. The permeability obtained by analysis will be a thickness-weighted average value (Horne, 1995).

This multilayer oil and gas scenario is for a small 'sandwich' of layers. These represent a small portion of the reservoir and experience similar pressures in the wellbore during the test. This scenario is not applicable to geothermal wells. The reality of geothermal wells is a large

number of permeable zones, of any orientation, distributed over the length of the open hole section, each of which experience different pressures in the wellbore during the test e.g. zones near the bottom of the well experience very high pressures during injection (flow is from the well into the reservoir) while zones at higher levels experience much less pressure (flow can be from the reservoir into the wellbore).

The significance of WK44/0 is that is it a small-scale simple example of the complex geothermal multilayered well issue. There are only two permeable zones in the well and the upper zone flows back into the well at a certain identifiable point during the test. The characteristic kink in the pressure data and small dip in the pressure derivative are diagnostic of a small inflow early in the PFO.

3.1.7 Semilog analysis

If the downflow scenario is temporarily ignored then semilog analysis (Miller et al., 1950) is possible. A reasonably flat derivative is present approximately 1.5 log cycles from the deviation of the derivative and the pressure in the derivative plot (Figure 4). The semilog straight line (Figure 11) gives a result of k = 0.67 mD and s = -4.87. This permeability is significantly less than for all the models of Table 1. The best model possible is Model 4 which gives a k of 2.26mD and so relative to this the semi-log analysis underestimates this by 70%.

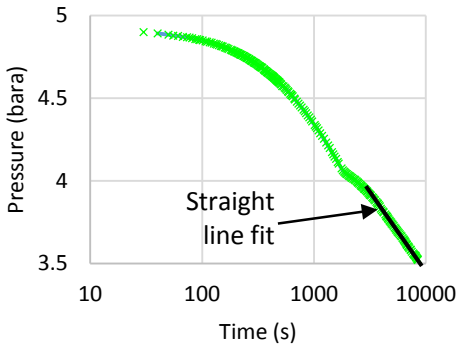

Figure 11: Invalid simplistic semilog analysis of dataset

The downflow renders the semilog analysis invalid. The straight line is fit to data that represents the superposition of both the PFO and the response to the downflow

3.1.8 Temperature and density effects

It is not a new concept that a downflow of fluid from a higher feed zone to a lower one will create issues for PTA. In fact this is discussed by Grant and Bixley (2011) as the most common reason for incorrect analyses for PTA involving injection. This is discussed by the authors in terms of the increase in temperature (due to inflows of hot fluid) and hence reduction of density of the fluid column.

Temperature change is not a concern for this particular test as the downflow is of cold injected water which was temporarily detained in the shallow permeable zone. This study fortunately has to consider only the change in mass in the wellbore.

3.1.9 Thought Experiment A

Moving beyond the field data it is interesting to consider a 'perfect' dataset generated using SAPHIR™ by retaining the parameters of Model 4 (Table 1) and extending the time history into the future. Taking this 'perfect' dataset as a starting point, downflows can be applied to see the effect they have on the derivative, semilog and history plot. Even more interesting is the effect the downflows have on the results of analysis. Figure 11 already shows what various downflow rates look like on a history plot. Figure 12 shows the same data in a semilog plot. These pressure histories can be input into SAPHIR™ and the derivative generated (Figure 13).

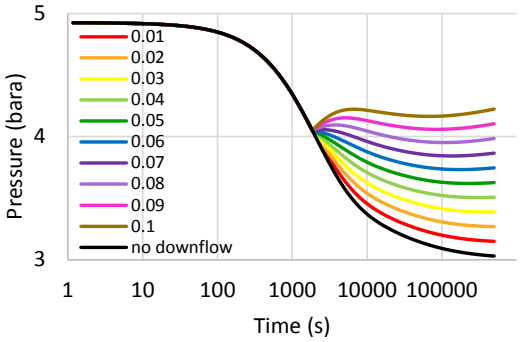

Figure 12: Semilog (MDH) plot for a range of downflows 0.01 – 0.1 m^3/h starting approximately after 31min into PFO.

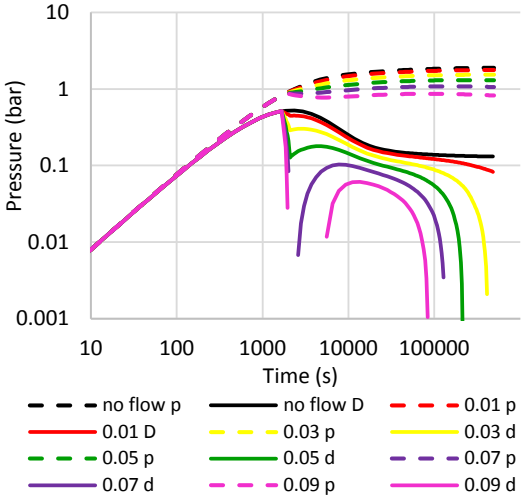

Figure 13: Derivative plot for a selection of downflows 0.01 – 0.09 m^3/h starting approximately after 31min into PFO.

Semilog analysis of these scenarios is possible (if not valid) if the kink in the dataset is ignored and the reservoir engineer is not rigorous is requiring a perfectly flat derivative and applying the 1.5 log cycle rule (Horne, 1995). It is plausible this may occur for low downflow rates and becomes less likely for high downflow rates where the distortion seen in the plots is more obvious. In practice datasets will often be noisy or too short and the distortions clear in Figures 10, 12 and 13 easier to overlook. Regardless of the likelihood of semilog and model analysis occurring in practice, the results for it are given in Table 2a and 2b.

It can be seen in Figure 12 that the negative slope at the end of the semilog plot will decrease, flatten and become positive as downflow rate increases. The result of this is a progressive overestimate of permeability and skin (Table 2a).

Table 2: Analyses of Thought Experiment A

'Perfect' dataset	k (mD)	k error (%)	s	s error (%)	Parameters of SAPHIR™ model
	2.26	-	-0.81	-	
a) Semilog analyses					
Downflow (m^3/h)	k (mD)	k error (%)	s	s error (%)	Comment
0	2.2	3	-1.02	26	Good line fit
0.01	2.41	7	-0.88	9	Good line fit
0.03	2.79	23	-0.84	4	Ok line fit
0.05	3.53	56	-0.33	59	Poor – kink and kick at end
0.07	4.62	104	0.30	137	Implausible – kink and kick at end
0.09	7.27	222	2.37	393	Implausible – kink and kick at end
b) Model fits (Infinite homogenous reservoir)					
0.01	2.44	8	-0.76	6	Good match except for late time drop
0.03	2.89	28	-0.61	25	OK match except for late time drop
0.05	3.9	73	0.41	151	Poor match especially derivative dip and late time drop
0.07	5.4	139	1.57	294	Very poor match especially derivative dip and late time drop
0.09	12.5	453	9.99	1333	Implausible

The semilog method applied to the perfect dataset gives results inconsistent with the perfect dataset parameters with a skin error of 26% (Table 2a). We must bear in mind that the semilog method depends on where exactly the reservoir engineer places the straight line. The results are highly sensitive to the slope of this line. Therefore the results of analysis in Table 2a are not exactly reproducible, though they provide a useful indication of the likely magnitude of error introduced by the downflows.

The errors from semilog analysis for both k and s increase non-linearly with downflow rate. The point at which they become significant depends upon what is considered as an acceptable level of error. Assuming this to be 20% then the errors exceed this level with even a small downflow of 0.03 m^3/h which is one-sixth of the original injection flow of 0.18 m^3/h.

The model fits (Table 2b) cannot match the derivative dip and late-time drop seen in Figure 14. Again the magnitude of error exceeds 20% with a 0.03 m^3/h downflow.

3.1.10 Thought Experiment B

It is interesting to consider how the effects change if the downflow comes in earlier (after 2 minutes). The effect of this on the shape of all the plots (Figure 14, 15 and 16) and the values of k and s are investigated (Table 3).

If the downflow begins early then it is barely noticeable in a history plot (Figure 14). For higher downflow rates the curve flattens earlier and at a higher pressure. For significant downflow rates (around 50% of the pre-PFO injection rate of 0.18 m^3/h) the pressure starts to increase towards the end of the test. These effects are more noticeable in a semilog plot (Figure 15).

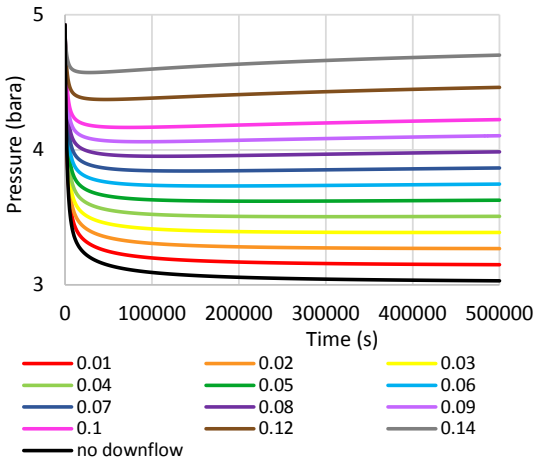

Figure 14: History plot for a range of downflows 0.01 – 0.14 m^3/h starting at 2 minutes into the PFO.

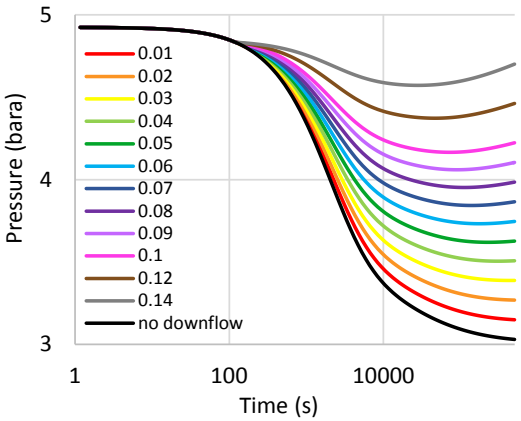

Figure 15: Semilog plot for a range of downflows 0.01 – 0.14 m^3/h starting at 2 minutes into the PFO.

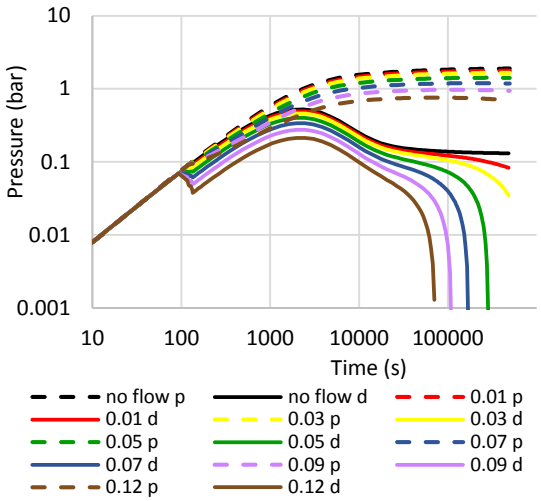

Figure 16: Derivative plot for a range of downflows 0.01 – 0.14 m^3/h starting at 2 minutes into the PFO.

The effect on the pressure derivative plot (Figure 16) is a small dip <0.5 log cycles wide. This is very small even for significant downflow rates and could easily be overlooked

in a real dataset with some noise. A more obvious sign is the continual decrease of the derivative instead of the flattening expected of the IARF regime. Even a very small downflow will prevent the derivative from flattening. For larger downflows this decrease is precipitous and resembles a constant-pressure response (Horne, 1995).

Table 3: Analyses of Thought Experiment B

'Perfect' dataset	k (mD)	k error (%)	s	s error (%)	Parameters of SAPHIR™ model
	2.26	-	-0.81	-	
a) Semilog analyses					
Downflow (m^3/h)	k (mD)	k error (%)	s	s error (%)	Comment
0.01	2.48	10	-0.69	15	Good line fit
0.03	2.45	8	-1.21	49	Good line fit
0.05	3.23	43	-0.39	52	Ok line fit
0.07	4.24	88	0.38	147	Poor – kick at end
0.09	6.31	179	2.1	359	Implausible – kick at end
b) Model fits (Infinite homogenous reservoir)					
0.01	2.46	9	-0.71	12	Good match except for late time drop
0.03	2.69	19	-0.57	30	Good match except for late time drop
0.05	3.14	39	-0.56	31	Good match except for late time drop
0.07	3.6	59	-0.80	1	Good match except for late time drop
0.09	4.08	81	-1.32	63	OK match except for late time drop

The error for k and s from semilog analysis (Table 3a) and model fits (Table 3b) exceed 20% for the same magnitude of downflow as Thought Experiment A (0.03 m^3/h). However in general the errors are lower in magnitude than for the same downflow applied in Thought Experiment A. The most important point from this experiment is that it would be much easier to perform an incorrect analysis with an early downflow as the effects on the derivative plot are more subtle. The derivative dip is small and the late-time drop would likely not be seen in a real, short dataset. If the late-time drop was observed it would likely be attributed to some kind of boundary effect. The results obtained if the presence of the downflow was overlooked would have significant errors even for small downflows.

3.1.7 Thought experiment C

It is interesting to consider what the effect is if the downflow comes in later, at 90 minutes. The effect of this on the shape of all the plots (Figure 17, 18 and 19) and the values of k and s is investigated (Table 4).

When the downflow starts at 90 minutes the effect is much more obvious on a history and semilog plots (Figures 17 and 18). On the derivative plot the dip is larger than that for an equivalent downflow at 2 minutes, and the precipitous drop occurs earlier in the test (Figure 19). The analysis has only been performed up to a downflow rate of 0.05 m^3/h as the effects of a late downflow are so much stronger.

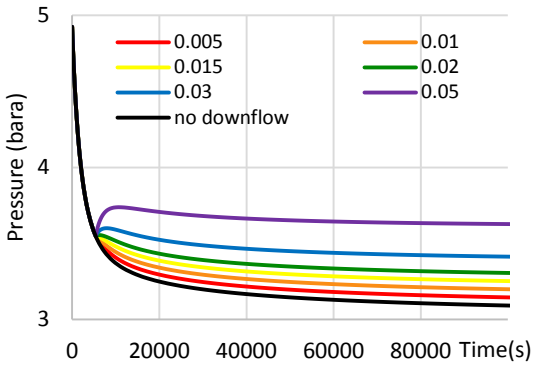

Figure 17: History plot for a range of downflows 0.01 – 0.05 m^3/h starting at 90 minutes into the PFO.

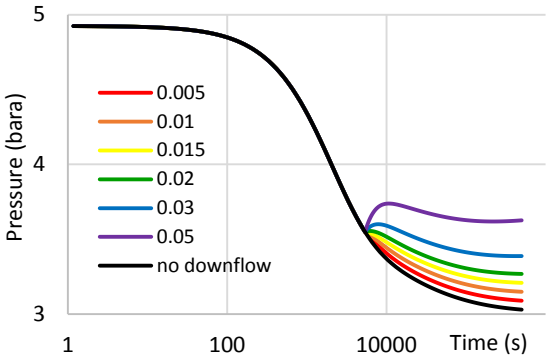

Figure 18: Semilog plot for a range of downflows 0.01 – 0.05 m^3/h starting at 90 minutes into the PFO.

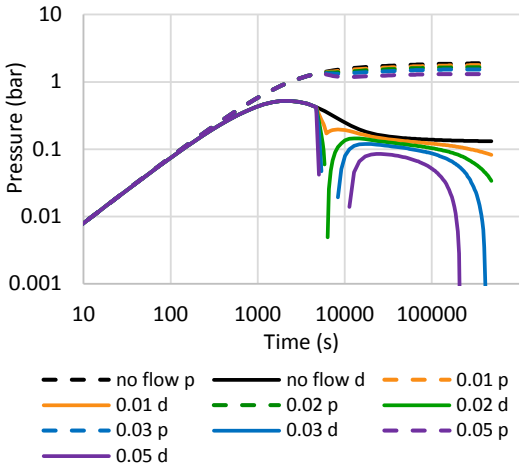

Figure 19: Derivative plot for a range of downflows 0.01 – 0.05 m^3/h starting at 90 minutes into the PFO.

Semilog analyses (Table 4a) and model fits (Table 4b) start as OK-poor matches and rapidly become implausible. The error exceeds 20% for k or s or both for all analysis in Table 4. The errors introduced by overlooking the downflows are much greater for a late downflow. However it becomes much more unlikely that downflow could be overlooked considering the obvious effects on the history, semilog and derivative plots (Figure 17, 18, 19).

Table 4: Analyses of Thought Experiment C

'Perfect' dataset	k (mD)	k error (%)	s	s error (%)	Parameters of SAPHIR™ model
	2.26	-	-0.81	-	
a) Semilog analyses					
Downflow (m^3/h)	k (mD)	k error (%)	s	s error (%)	Comment
0.01	2.05	9	-1.82	125	Poor line fit, kink obvious and kick at end
0.02	2.35	4	-1.44	78	Poor line fit, kink obvious and kick at end
0.03	2.73	21	-0.97	20	Very poor line fit, kink obvious and kick at end
0.05	3.7	64	0.04	105	Implausible
b) Model fits (Infinite homogenous reservoir)					
0.01	2.79	23	0.21	126	OK match except for late time drop and derivative dip
0.02	3.46	53	1.43	277	Poor match especially late time drop and derivative dip
0.03	4.49	99	3.3	507	Poor match especially late time drop and derivative dip
0.05	8.43	273	10	1335	Implausible

3.2 ISSUE 2: NON-ZERO FLOW EARLY IN PFO

3.2.1 Description of the non-zero flow issue

A very common issue in injection/PFO tests is that the shutdown of injection flow is achieved only by closing the master valve. This can take a few minutes at best and up to 10 minutes. The result is a dataset where the PFO is rounded, either smoothly in the case of a smoothly-closing valve (e.g. WK317, Figure 20) or incrementally in the case of a valve closed by increments (WK318, Figure 20).

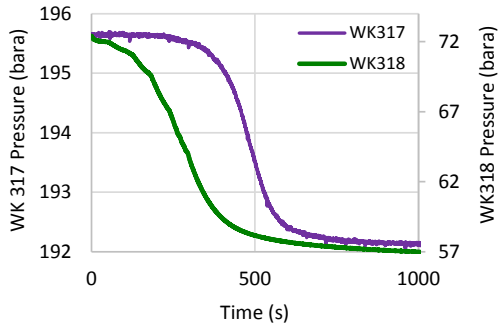

Figure 20: Rounded PFO datasets for WK317 and WK318 (first 1000s).

The effect of this rounding of the dataset is to produce a log-log plot that rises too steeply in early time and is scattered (Figure 21) or with multiple humps (Figure 22). In either case it is not possible for analytical models to match this shape.

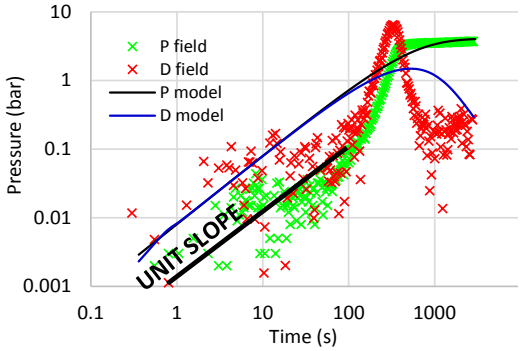

Figure 21: WK317 derivative plot of smoothly rounded PFO

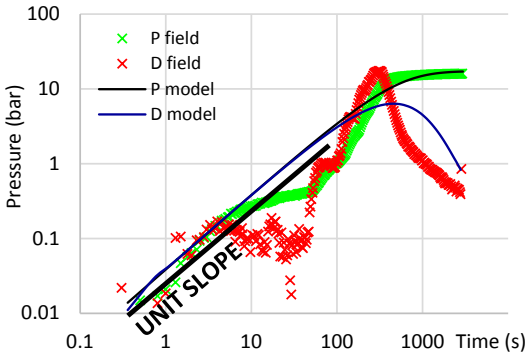

Figure 22: WK318 derivative plot of incrementally rounded PFO

3.2.2. Manipulation of the dataset to remove rounding

The accepted method of dealing with this issue (Contact Energy, personal communication) is illustrated in Figure 23. The first point at which the pressure starts to decrease is retained, then the data is cut away until the PFO appears to be 'clean' and dropping steeply in the usual manner, then the remaining PFO data is time-shifted until it lines up with the initial point. The intervening space is filled with a straight line of pressure dropping linearly with time. This artificial early-time data is required as the reservoir engineer will struggle to fit any analytical models if there is no early-time data.

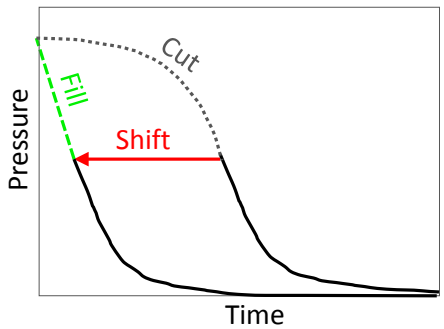

Figure 23: Show the removal of the rounded portion of the dataset, time-shifting and linear data-filling.

This method is accepted as it is the only way to fit an analytical model to the dataset. Alternatively the rounding could be ignored and a semilog straight line fit to the end of the dataset. However the degree to which the final results are affected by either method of analysis is not known.

3.2.3 Results for original and manipulated datasets

Ignore the distortion – semilog analysis

It is not possible to simply ignore this issue and simply fit an analytical model due to the distorted shape of the dataset (Figures 21 and 22).

Semilog analysis is a poor option, if a flat section of derivative is present at all. Also the distortion of the dataset makes it impossible to determine the point at which the derivative deviates from the pressure to apply the 1.5 log cycle rule (Horne, 1995).

Semilog analysis of WK317 gave k = 1550 mD and s = 3.36. This is on a section of data that appears reasonably flat on a derivative plot, despite lots of noise. For WK318 semilog analysis not possible as the derivative continues to decrease to the end of the dataset.

Manipulate the dataset

The WK317 dataset has been manipulated by the cut-shift-fill method as described in Section 3.2.2. The results from analytical model fits are very sensitive to where the data is cut and the time-shift applied. Various scenarios have been created with a range of cut points and time-shifts, some of which are represented in Figure 24. The dataset is cut in one of two places: firstly where it appears flat to the naked eye on a history plot (290s), and secondly at the inflexion point (340s). A range of time-shifts are then applied to each as detailed in Table 5. The results from analytical model fits and semilog analysis of these scenarios are given in Table 5. Derivative plots of the scenarios are given in Figure 25 and 26.

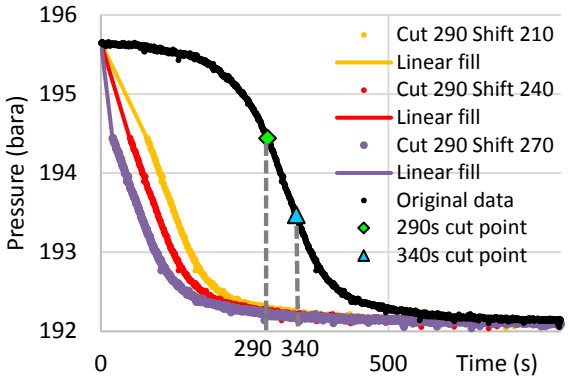

Figure 24: Range of scenarios for cutting, shifting and filling the WK317 dataset. Two cut points 290s and 340s shown as well as the range of time-shifts for the 290s cut point (210s, 240s and 270s).

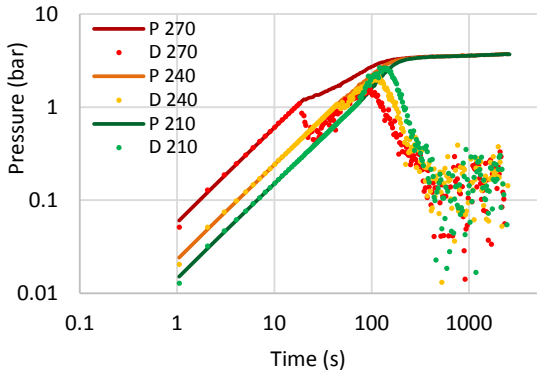

Figure 25: Derivative plots for datasets cut at 290s.

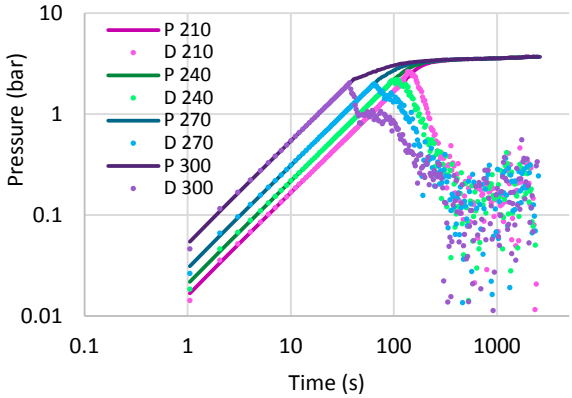

Figure 26: Derivative plots for dataset cut at 340s.

Table 5: Results for cut-shift-fill scenarios

Scenario	SAPHIR model fit (units k: mD)	Semilog (units k: mD)
Cut 290 Shift 210	Peak steepest. Poor fit. k=7260, s=48.8	k=1950 s=6.39
Cut 290 Shift 240	Peak still steep. Poor fit. k=7410, s=48.8	k=1850 s=5.69
Cut 290 Shift 270	Step in peak but otherwise more reasonable shape k=4910, s=28.8	k=2260 s=8.7
Cut 340 Shift 210	Struggles to match peak and steep drop k=9480, s=66.3	k=2090 s=7.4
Cut 340 Shift 240	Struggles to match peak and steep drop k=7470, s=49.5	k=2060 s=7.17
Cut 340 Shift 270	Peak and drop not so steep but match still poor k=6920, s=44.7	k=2310 s=9.07
Cut 340 Shift 300	Overall slope improved, peak shallower but with step in top, otherwise match OK k=3640, s=19.8	k=2190 s=8.18
Uncorrected	n/a no question of being able to match this dataset	k=1540 s=3.27

It can be seen from the results (Table 5) that:

- Model match is still poor even after manipulation as the steep peak remains, though it is less steep than before.
- The steepness of the peak decreases with increasing time-shift.
- If the time-shift goes “too far” the derivative exhibits a dip.
- The model matches (although a poor match in shape especially for the steeper peaks) exhibit a wide range of k 3640-9480 mD and s 19.8-66.3.
- Generally k and s decrease as the time shift increases.
- All values seem unreasonably high. The smallest value for s is 19.8, which for a geothermal well stimulated by injection is highly unlikely.

- Semilog results range k 1850-2310 mD and s 5.67-9.07 which are more consistent with each other.
- All scenario semilog results are higher than the semilog results for the uncorrected dataset k 1540 mD and s 3.27.

Because we do not know what the 'truth' is we have no way to quantify the accuracy (or otherwise) of the results. However observations of importance are:

- With increasing time-shift the derivative becomes a more reasonable shape with a gently rounded hump rather than a steep peak. This improves the model match and returns the lowest values for k and s.
- With increasing time-shift a small dip/step appears in the early part of the derivative. This is a mismatch between the slope of the linear fill and the slope of the real data and is not significant.
- Applying a time-shift carefully so there is no significant difference in slope at the join between the linear fill and the real data will produce a derivative that has no step. This derivative might still have a quite steep peak.
- The most plausible results come from the scenario cut at the inflexion point and with the largest time-shift.

3.2.4 Thought experiment D

The trouble with quantifying the effect something has on the results is that there is no way to know what those results "should be" for a real well. Therefore it is of interest to generate a 'perfect' dataset with known well and reservoir parameters. The rounded-PFO effect is then recreated with that dataset and analysed to see how the known parameters are affected.

Two 'perfect' datasets are created based on the injection/PFO tests of WK317 and WK318. The models used are the simplest case of homogenous/infinite reservoir with storage and skin. Though SAPHIR™ is not a forward modelling program and it needs something to match, once this match is done (however poor) those model parameters can be retained and used for forward modeling by changing the injection history far into the future. For these datasets the injection flows of the original PFO test have be replicated at a time of 1E+6s into the future. This is far enough in the future to not affect the model match. The critical difference of the replicated future PFOs is that the cessation of injection is not an instantaneous drop to zero (as is commonly assumed for the purposes of modelling) but rather an incremental decrease of the flow of 10% of the initial value at 30s intervals.

These incremental PFOs are successful at creating rounded pressure histories (Figure 27) and derivative peaks that are too steep (Figure 28, 29).

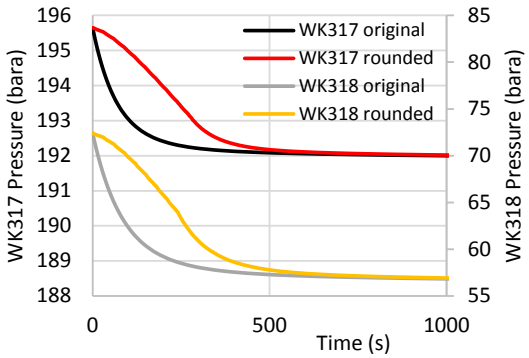

Figure 27: Model based on WK317. Black line shows modelled PFO based on instantaneous shut. Red line shows PFO based on incremental shut.

The datasets were given the cut-shift-fill treatment as described in Section 3.2.2 with the cut made at the inflexion point and the time-shift applied to match the slope of the linear fill to the real data.

WK317 model results

The derivative plot (Figure 28) shows the original perfect dataset, the distortion resulting from the incremental PFO and the correction of the cut-shift-fill treatment. The results of analysis are given in Table 6.

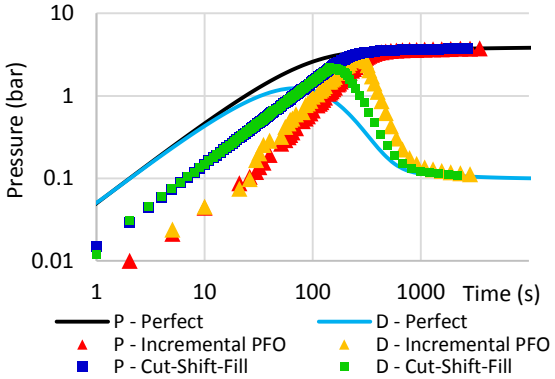

Figure 28: Derivative plot of WK317 thought experiment comparing the perfect dataset (black and blue lines) to the distortion caused by incremental PFO (red and yellow squares) and correction using the cut-shift-fill method (blue and green squares).

Table 6: Results for WK317 model

'Perfect' dataset	k (mD)		s	
	2370		10	
a) Semilog analysis of perfect dataset				
	k (mD)	Error %*	s	Error %
Semilog (good fit of straight line)	2300	3	9.46	5
b) Incremental PFO distortion				
Model match (very poor match of steep peak)	3450	46	20	100

Semilog (good match)	1850	22	5.94	41
c) Cut-shift-fill correction				
Model match (poor match of steep peak)	2280	4	10	0
Semilog (good match)	2080	12	7.71	13

*error is calculated as a % compared to the 'truth' which is the parameters from the 'perfect' dataset.

Observations:

- The 'truth' of the perfect dataset is closely recreated by the semilog method with k error 3% and s error 5%.
- The distorted incremental PFO dataset has the steepest peak.
- This dataset has a very poor match with a SAPHIR model due to the steep peak, which overestimates k and s (errors 46% and 100%).
- The semilog method applied to this dataset has a good match but underestimates k and s significantly (errors 22% and 41%).
- The cut-shift-fill correction partially restores the original shape of the derivative plot (Figure 28).
- The model match is still not good due to the steep peak however regardless of this the results for k and s generated are consistent with the perfect dataset (errors 4% and 0%)
- The results from semilog analysis of this corrected dataset are also improved though are still higher than the original semilog analysis (12% and 13%).

WK318 model results

The derivative plot (Figure 29) shows the original perfect dataset, the distortion resulting from the incremental PFO and the correction of the cut-shift-fill treatment. The results of analysis are given in Table 7.

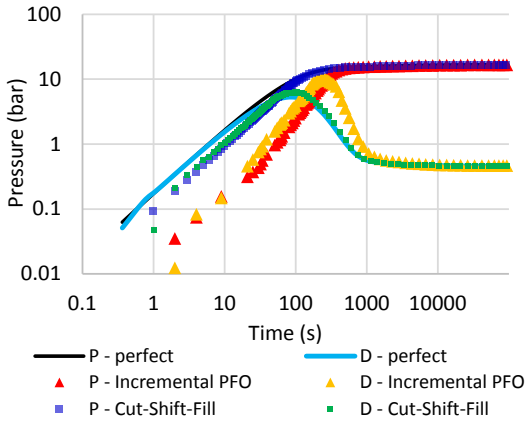

Figure 29: Derivative plot of WK318 thought experiment comparing the perfect dataset (black and blue lines) to the distortion caused by incremental PFO (red and yellow squares) and then the attempt at correction using the CSF method (blue and green squares).

Table 7: Results for WK318 model

'Perfect' dataset	k (mD)		s	
	1000		9.36	
a) Semilog analysis of perfect dataset				
	k (mD)	Error %*	s	Error %
Semilog (good fit of straight line)	967	3	8.69	7
b) Incremental PFO distortion				
Model match (very poor match of steep peak)	2110	111	29.2	212
Semilog (good match)	964	4	8.64	8
c) Cut-shift-fill correction				
Model match (good match)	1030	3	9.95	6
Semilog (good match)	939	6	8.21	12

*error is calculated as a % compared to the 'truth' which is the parameters from the 'perfect' dataset.

Observations:

- The correction in this case returns the derivative shape to one hard to distinguish from the original (Figure 29). The results for k and s are very close to the 'truth' (errors 3% and 6%)
- In all cases the semilog method here gives a reasonable approximation of the 'truth' (errors 3-12% on k and s)
- Analysis of the distorted incremental PFO gives a very poor match with a SAPHIR model due to the steep peak, which overestimates k and s massively (errors 111 and 212%).

Observations from both perfect datasets

For the two 'perfect' datasets the model results are massively overestimated by the distortion introduced by the rounded PFO, and then returned to reasonable values (within a few % error) by the cut-shift-fill correction.

The results for the semilog method are more varied. For WK318 the results were hardly affected by the distortion and correction (error for all results <12%) while for WK317 the results went from reasonable (k and s errors 3 and 5%) to unreasonable (22 and 41%) and then slightly improved but still not acceptable (12 and 23%).

5. CONCLUSIONS

5.1 Downflows

The characteristic pressure derivative produced by a downflow is a small dip <0.5 log cycles wide when the downflow starts. This dip is not very noticeable when it occurs early in the PFO and the pressure is changing the most rapidly. It is more obvious later in the PFO when the pressure is changing more slowly.

The derivative will also not reach a constant value, instead it will drop away in intermediate-late time in a manner resembling a constant-pressure derivative. This steep drop will only be observed if the dataset is sufficiently long.

As a model fit must be made on a drastically reduced dataset (only data prior to start of downflow) it is very important to obtain a value for Pi as this will provide an important constraint for the model.

Any semilog analyses of datasets with downflows are technically invalid as all the data used is affected by the downflow.

For a downflow that is even a small fraction of the injection flow (one-sixth), the values of k and s are overestimated by both model fits and semilog analysis beyond a reasonable level of error of 20%.

A downflow of the same magnitude will produce a greater error if it commences in late time compared to early time. However the presence of late downflows is more obvious in history, semilog and derivative plots and so invalid analysis is more unlikely. Caution should be taken to look for early downflows as their effect could be overlooked even in a derivative plot, though the impact on results for k and s is significant.

5.2 Non-zero flow

The pressure derivative anomaly produced by non-zero flow early in the PFO is a shift in the unit slope to the right and a steep rise into a sharp peak which then drops too steeply down to the flat derivative section. This overall basic shape may also be scattered or humped.

If this effect is ignored and a standard analysis is performed, the result will be a very poor model match if any (no model can match this steep peak) and results for k and s that are massively overestimated. While semilog analysis might seem the best option as there is still a semilog straight line present it also has the potential for significant error, though to a lesser extent than model matching.

When attempting to remove this effect by applying the cut-shift-fill correction the results from model matching are returned to very close to the true values, within a few %. For semilog analysis the results do not necessarily improve with application of the cut-shift-fill method.

The exact manner in which the cut-shift-fill correction is applied will drastically affect the results obtained from subsequent analysis of the dataset. The data should be cut at the inflexion point and time-shifted to match the slope of the linear fill to the real data. The application of the method in this manner has produced results in both synthetic data thought experiments which are within a few % of real values.

6. ACKNOWLEDGEMENTS

The authors kindly acknowledge Contact Energy for access to well test data and resources.

7. REFERENCES

Bourdet, D., Whittle, T.M., Douglas, A.A., and Pirard, Y-M.: *A New Set of Type Curves Simplifies Well Test Analysis*. World Oil, May, 95-106 (1983).

Bourdet, D., Ayoub, J.A., and Pirard, Y-M.: *Use of Pressure Derivative in Well Test Interpretation*. SPE Formation Evaluation, June, 293-302 (1989).

Bourdet, D.: *Well Test Analysis: The Use of Advanced Interpretation Models*. Handbook of Petroleum Exploration and Production 3 (2002).

Earlougher, R.C., Jr.: *Advances in Well Test Analysis*. Society of Petroleum Engineers Monograph 5, Dallas, Texas (1977)

Grant, M.A. and Bixley, P.F.: *Geothermal Reservoir Engineering*. 2nd ed., Elsevier Inc. (2011)

Horne, R.N.: *Modern Well Test Analysis: A Computer-Aided Approach*. 2nd Ed. Petroway Inc (1995)

Houzé, O., Viturat, D. and Fjaere, O.S.: *Dynamic Data Analysis.* KAPPA Engineering electronic book (2012)

Miller, C.C., Dyes, A.B., Hutchinson, C.A.: *The Estimation of Permeability and Reservoir Pressure from Bottom-hole Pressure Build-up Characteristics*. Trans AIME, 189 (1950).

O'Sullivan, M.J., Croucher, A.E., Anderson, E.B., Kikuchi, T. and Nakagome, O.: *An Automated Well-Test Analysis System (AWTAS)*. Geothermics, vol 34(1) pp 3-25 (2005)